Lattice dynamics of solid α- and γ-N_2 crystals at various pressures

Eduardo Huler
Department of Inorganic and Physical Chemsitry, Soreq Nuclear Research Centre, Yavne, Israel

Alex Zunger*
Department of Theoretical Physics, Soreq Nuclear Research Centre, Yavne, Israel
and Department of Chemistry, Tel Aviv University, Tel-Aviv, Israel
(Received 31 March 1975)

A previously published interaction potential between N_2 molecules has been utilized to compute the lattice mode frequencies of solid α- and γ-N_2 at the equilibrium crystal structure corresponding to various pressures. Dispersion curves and the density of states are given. These are then used to calculate the lattice heat capacity, Grüneisen mode parameters throughout the Brillouin zone, linear thermal-expansion coefficient, Debye temperatures, and temperature-dependent root-mean-square amplitudes of vibrations. Whenever comparison with experimental data is possible, good agreement is obtained.

I. INTRODUCTION

Lattice-dynamics calculations, which have been carried out extensively on atomic crystals, have been extended recently to the study of molecular crystals.[1-6] This is mainly due to the accumulation of extensive experimental data on properties of molecular solids that are determined by the phonon dynamics, such as Raman and infrared spectra, coherent and incoherent neutron scattering, heat capacity, amplitude of vibrations, thermal expansion, and high-pressure Raman spectra. Using an explicit form for the intermolecular potential, it is possible to calculate not only lattice-dynamical properties but also the equilibrium crystal structure corresponding to various crystal phases and the lattice cohesive energy.

In a previous paper[5] it has been shown that an explicit atom-atom potential is suitable for reproducing Raman and infrared frequencies, and unit-cell parameters of α- and γ-N_2 crystals, cohesive energy of α-N_2, and virial coefficients for gaseous N_2 which are in agreement with experimental results. It has been shown that special care must be taken in the minimization of the crystal energy with respect to structural parameters in order to avoid erroneous results in the calculation of lattice frequencies. The effect of zero-point energy and convergence of the lattice sums of the calculated structure and lattice frequencies, were also investigated. It is the aim of the present paper to extend these studies to properties which depend on the detailed dynamical spectrum through the Brillouin zone, such as mean-square amplitudes of vibration, heat capacity, dispersion curves, density of lattice modes, and thermal expansion. The effect of pressure on some of these properties will also be examined.

II. LATTICE-DYNAMICS CALCULATION

The $3\sigma\tau$ vibrational frequencies $\omega_j(\vec{k})$ of a crystal containing σ molecules in the unit cell, each having τ atoms, are obtained for a given value of the wave vector $\vec{k}$, by solving the secular equations

$$\left| D_{\lambda\lambda'}(ss' \left| tt' \right| \vec{k}) - \omega_j(\vec{k})\delta_{\lambda\lambda'}\delta_{tt'} \right| = 0, \tag{1}$$

where λ and λ' denote Cartesian components, s and s' label the molecules in the unit cell ($s = 1 \cdots \sigma$), and t and t' denote the atoms ($t = 1 \cdots \tau$). The branch index j ranges from 1 to $3\sigma\tau$. The dynamical matrix has elements given

$$D_{\lambda\lambda'}(ss' \left| tt' \right| \vec{k}) = \frac{1}{(\sqrt{M_t M_{t'}})} \sum_{l'=1}^{N} \phi_{\lambda\lambda'}(lst, l's't') \times e^{i\vec{k}\cdot[\vec{R}(l)-\vec{R}(l')]}, \tag{2}$$

where M_t and $M_{t'}$ denote masses, l and l' label the unit cells ($l = 1 \cdots N$), and $\vec{R}(l)$ denotes the position of the unit cell relative to the origin. The force constants are given

$$\phi_{\lambda\lambda'}(lst, l's't') = \frac{\partial^2 \phi_s}{\partial u_\lambda(lst)\partial u_{\lambda'}(l's't')} . \tag{3}$$

$u_\lambda(lst)$ denotes the displacement in the λ direction of the atom t in molecule s located at unit cell l. The static interaction potential Φ_s is a sum of intermolecular (Φ_{inter}) and intramolecular (Φ_{intra}) terms:

$$\Phi_s = \Phi_{\text{inter}} + \Phi_{\text{intra}}. \tag{4}$$

No assumptions about the rigidity of the molecules are made. The intermolecular potential is given

$$\Phi_{\text{inter}} = \frac{1}{2} \sum_{st} \sum_{s't'} \sum_{l'} V_{\text{inter}}(D^{0,l'}_{st,s't'}), \tag{5}$$

where $V_{\text{inter}}(D^{0,l'}_{st,s't'})$ is the assumed atom-atom interaction potential between atoms t belonging to a molecule s located in a central unit cell ($l = 0$) and atom t' of the molecule s', located in unit cell l'. $D^{0,l}_{st,s't'}$ denotes the corresponding atom-atom distance. The intramolecular potential is

$$\Phi_{\text{intra}} = \sum_{s} \sum_{t} \sum_{t'} V_{\text{intra}}(D^{0,0}_{st,st'}), \tag{6}$$

where $D^{0,0}_{st,st'}$ denote intramolecular atom-atom distances. The self-term in the dynamical matrix is calculated using the constraint of invariance of the potential energy with respect to an over-all translation of the particles in the system,[7] i.e.,

$$\Phi_{\lambda\lambda'}(lst, lst) = -\sum_{l's't' \neq lst} \phi_{\lambda\lambda'}(lst, l's't'). \tag{7}$$

The constraints which have to be imposed on the dynamical matrix due to the lattice symmetry and the invariance of the lattice sums with respect to the choice of the origin, are automatically accounted for in our computational scheme owing to the explicit calculation of the force constants from the interaction potential.

In the computational scheme employed the calculation of the lattice dynamics is carried out in the following way: An initial crystal configuration is generated by assuming the values of the unit cell parameters a, b, c, α, β, and γ and the positions of the τ atoms in one of the σ molecules in the central unit cell. The positions of the rest of the atoms in the crystal are generated by applying symmetry operations of an assumed space group to this initial configuration. The positions of the $\sigma\tau$ atoms in the unit cell and the values of the unit-cell parameters at static equilibrium are obtained from the solution of the set of equations

$$\nabla_{\vec{r}_x}\Phi_s = 0, \quad x = 1 \cdots \sigma\tau, \tag{8a}$$

$$\nabla_{\vec{R}_p}\Phi_s = 0, \quad p = 1 \cdots 6, \tag{8b}$$

where $\vec{r}_x$ is the position vector of atom x in the unit cell while the $\vec{R}_p$ ($p = 1 \cdots 6$) are the 6 unit-cell parameters. This set of equations is solved iteratively using steepest-descent and Newton-Raphson minimization techniques without imposing any symmetry restrictions on the minimization path. The lattice sums in Eqs. (5) and (6) are examined to be convergent (interactions are summed up to 25 Å). The dynamical eigenvalue problem [Eq. (1)] is solved at the unit-cell parameters and atomic positions which satisfy Eq. (8). Since the crystal interaction potential Φ [Eqs. (4)–(6)] is strongly anharmonic, the elements of the dynamical matrix given in Eq. (3) depend on both the unit-cell parameters (which determine the volume per molecule) and the atomic positions inside the unit cell. Relaxation of all the forces and torques exerted on the molecules [Eq. (8a)] is necessary for obtaining the lattice frequencies $\omega_j(\vec{k})$ in a way which is consistent with the potential adopted. In simple atomic crystals (e.g., fcc, bcc) the symmetry of the lattice already assures the vanishing of forces on the atoms.

The effect of zero-point energy on the lattice conformation is introduced in the second step of the calculation where we minimize the total interaction potential Φ_{tot} rather than the static part Φ_s:

$$\Phi_{tot} = \Phi_s + \Phi_{zp}. \tag{9}$$

The minimizing conditions are given

$$\nabla_{\vec{r}_x}\Phi_{tot} = 0, \tag{10a}$$

$$\nabla_{\vec{R}_p}\Phi_{tot} = 0. \tag{10b}$$

Φ_{zp} denotes the zero-point energy, calculated from the density of states $D(\omega)$:

$$\Phi_{zp} = \frac{h}{2}\int_0^\infty D(\omega)\, d\omega. \tag{10c}$$

The density of states is obtained (see below) from the eigenvalues $\omega_j(\vec{k})$ calculated in the previous step, using the interpolation scheme of Gilat and Raubenheimer.[8] A channel width of 0.25 cm^{-1} is employed and 800-$\vec{k}$-grid points are used. At the conformation obtained after solving Eqs. (10), we repeat the dynamical calculation. This cycle is repeated until the conformation and lattice spectrum are stabilized. The calculated dynamical properties reported here for the zero-pressure α-N_2 phase, correspond to this final step in the computation scheme. The calculations on the high-pressure γ-N_2 phase and on the α-N_2 at $P \neq 0$ are performed by solving Eqs. (8a) and (10a) for a given molar volume. The value of $-\nabla_{\vec{R}_p}\Phi_{tot}$ is now related to the external pressure that corresponds to these volumes at a dynamical equilibrium.

In the previous work[5] the intermolecular potential Eq. (5) was approximated by a Lennard-Jones type of interaction:

$$V_{inter}(D^{0,l'}_{st,s't'}) = \epsilon\left[\left(\frac{\sigma}{D^{0,l'}_{st,s't'}}\right)^{12} - \left(\frac{\sigma}{D^{0,l'}_{st,s't'}}\right)^{6}\right]. \tag{11}$$

The parameters σ and ϵ have been fitted through a least-square procedure to reproduce the experimental unit-cell dimensions,[9,10] the cohesive energy,[11,12] and the infrared[13,14] and Raman[15–17] frequencies of α-N_2 at $\vec{k} = 0$. This yielded

$$\sigma = 3.30 \text{ Å},$$

$$\epsilon = 0.30 \text{ kcal/mole},$$

where the intramolecular bond length was kept fixed at the experimental value of 1.098 Å.

For the intramolecular interaction [Eq. (6)], we have adopted the form suggested by Levine from the vibrational analysis of isolated N_2 molecule,[18]

$$V_{intra}(d) = D_e[1 - d_0/d]\,[e^{-\beta(d^p - d_0^p)}]^2, \tag{12}$$

where d_0 is the intramolecular bond length, $d \equiv D^{0,0}_{st,st'}$, D_e is the molecular dissociation energy, and p and β are parameters given by Levine. The exact form of the intramolecular potential does not affect the lattice modes because of the large energy separation between internal and external modes (the lowest molecular frequency is around 2300 cm^{-1} and the highest lattice frequency is 110 cm^{-1}).

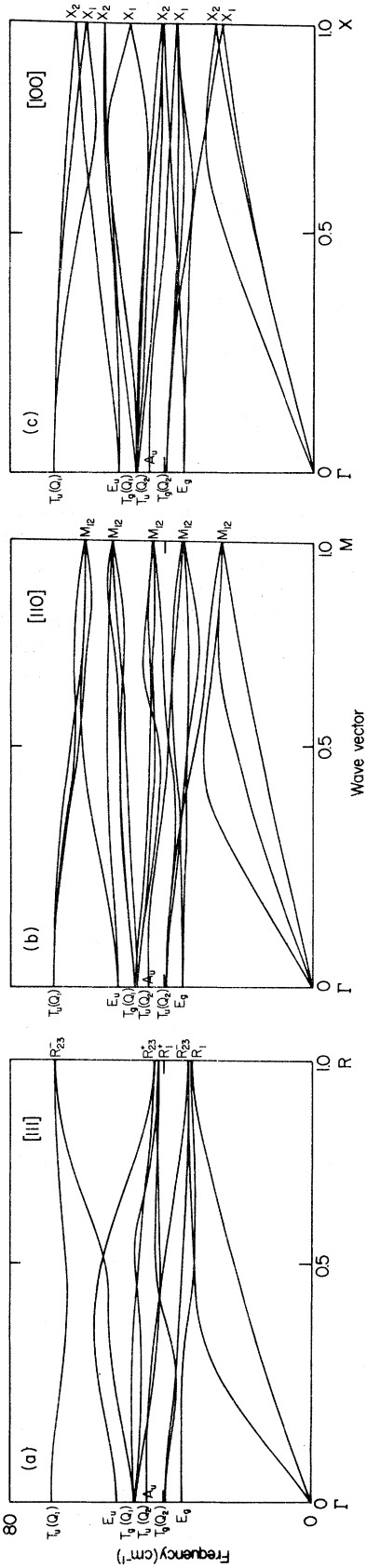

FIG. 1. Dispersion curves for α-N_2 at zero-pressure volume. (a) [111] direction; (b) [110] direction; (c) [100] direction.

III. DISPERSION CURVES

Dispersion curves for α-N_2 and γ-N_2 were calculated by solving the dynamical equations at 30 points in the Brillouin zone (BZ) along each of the directions considered. The dispersion curves for α-N_2 (space group $Pa3$, four molecules per unit cell) are given in Fig. 1 at the unit-cell dimensions corresponding to the equilibrium under normal pressure (molar volume 27 cm^3) predicted by the employed potential. These are compared with the experimental coherent inelastic neutron scattering of Kjems and Dolling[19] (Table I). The calculated dispersion curves are generally in good agreement with the observed values. The agreement between the experimental and calculated highest optical-mode frequencies (longitudinal optical) suggest that the rigid-ion approximation used here is reasonable and electronic polarization effects are not too important. This is to be contrasted with the situation in ionic solids where rigid-ion models overestimate considerably the frequency of the highest optical modes.[21] In Fig. 2 the dispersion curve along the [111] direction and for molar volumes of 24.1 and 27.2 cm^3, are given. The experimental α-to-γ

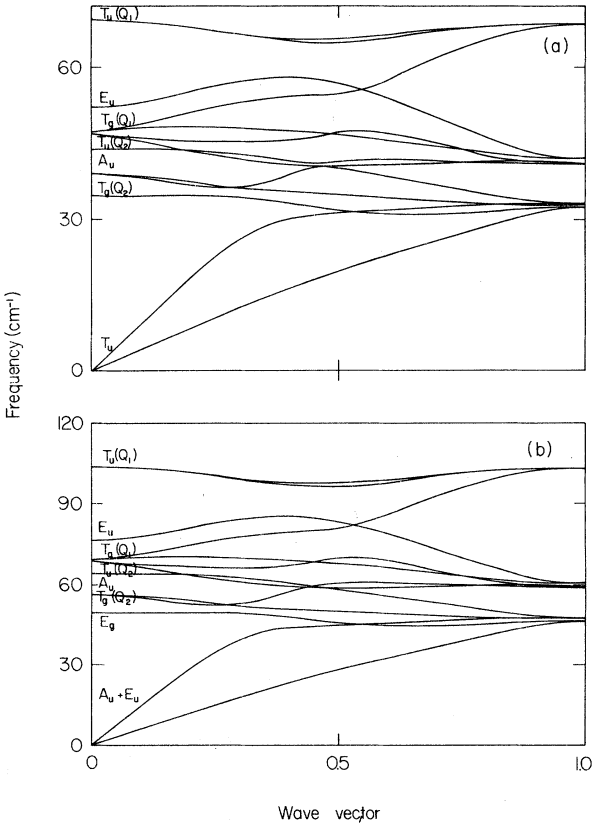

FIG. 2. Dispersion curves for α-N_2. (a) Molar volume 27.2 cm^3 (zero pressure); (b) molar volume 24.1 cm^3 (4 kbars).

TABLE I. Comparison between calculated and measured inelastic-neutron-scattering (Ref. 15) lattice frequencies at high-symmetry points in the Brillouin zone. The values in parenthesis correspond to the optical measurements (Refs. 13–16). Values given in cm^{-1}.

Γ Point		M Point		R Point		X Point	
Calc.	Obs.	Calc.	Obs.	Calc.	Obs.	Calc.	Obs.
69.5	69.60 (70.0)	61.2	62.7	68.4	68.7	63.7	
47.5	60.0 (60.0)						
51.8	54.20	53.7	55.0	42.0	47.3	60.9	
47.0	48.56 (36.0)	42.9	46.9	40.8	43.7	56.1	
43.7	46.92	34.7	38.0	32.9	34.8	49.3	44.5
38.5	36.42 (36.0)	24.6	27.9	32.2	33.9	40.8	
34.5	32.37 (31.5)					40.5	
						36.7	38.0
						36.5	
						26.5	
						24.01	27.5

phase transition was observed[10,20] at a volume of 24.1 cm^3 at 20.5 °K.[10]

It can be seen that the dispersion of the curves is only slightly affected by increasing the pressure. The frequencies of the optical branches are shifted quite homogeneously to higher values, while the highest acoustic mode is shifted strongly only for $\vec{k} < 0.5$ and much less for higher $\vec{k}$-values. The dispersion curves obtained in our calculations are similar in shape to those obtained by Ron and Schnepp[22] using a different 6-12 potential, and to those obtained by Raich *et al.*[23] using a self-consistent phonon treatment. One significant difference between our results and those of Ron and Schnepp is the removal of the accidental degeneracy at the R points in the present calculation. On the other hand, our calculations and those of Ron and Schnepp[22] and Raich *et al.*[23] differ significantly from the recent calculations of Kjems and Dolling.[19] The erratic behavior of the dispersion curves obtained by the latter probably result from the inadequacy of the renormalization between translational and librational modes at general $\vec{k}$ points.

Dispersion curves for γ-N_2 (space group D_{4h}^{14}, two molecules per unit cell) at the unit-cell parameters $a = b = 3.94$ Å, $c = 5.08$ Å corresponding to the calculated equilibrium structure under an external pressure of 4015 atm (experimental data[10] $a = b = 3.957$ Å, $c = 5.109$ Å under the same pressure) are shown in Fig. 3 along several directions. [In our previous work (Ref. 5), we have erroneously interchanged the assignment of the B_{1g} and A_{2g} librational modes of α-N_2 (Table VIII therein). The correct order is revealed in Fig. 3 here. We are grateful to Professor J. C. Raich for bringing this point to our attention.] The assignment of the branches were made by studying the transformation properties of the eigenvectors and using the noncrossing rule for branches of the same symmetry. Up to the present time, no experimental neutron-diffraction data is available for comparison with the calculated results for γ-N_2. The agreement between calculated and optically observed frequencies at $\vec{k} = 0$ is satisfactory.[5] Recently, Pawley *et al.*[24] have reported a calculation on γ-N_2 at $\vec{k} = 0$ using a $e^{-r^{-6}}$ potential. The results are qualitatively similar to our results, however better quantitative agreement is obtained in the present calculation with the 12-6 potential.

The dispersion of the Grüneisen parameters $\gamma_j(\vec{k})$

$$\gamma_j(\vec{k}) = -\frac{d \ln \omega_j(\vec{k})}{d \ln V} \tag{13}$$

were calculated numerically from the dispersion curves at several volumes. Some representative results obtained for the three acoustical modes and two of the optical modes (one a pure translational mode and the other a pure rotational mode at $\vec{k} = 0$) along the [111], [110], and [100] directions in α-N_2, are shown in Fig. 4. The acoustical nondegenerate Au mode has the highest Grüneisen parameter at $\vec{k} = 0$. Around $\vec{k} = 0.5$ along the [111] and [110] and around $\vec{k} = 0.7$ along the [100] direction, the Grüneisen parameter drops strongly, indicating the softening of this mode. The other acoustical-mode parameters as well as the optical-mode parameters exhibit low dispersion. The mode parameters of branches that are degenerate at $\vec{k} = 0$ and nondegenerate at higher $\vec{k}$ values, differ only slightly. The agreement between observed[25,26] and calculated Grüneisen mode parameters at $\vec{k} = 0$ is quite poor.[5] The addition of interaction terms falling with distance slower than the 12-6 potential (e.g., quadrupole-quadrupole) would lower the calculated values[27] thus bringing them to better agreement with experiment.

IV. DENSITY OF STATES

The $\vec{k}$-space interpolation scheme of Gilat and Raubenheimer[8] was used to obtain the normalized

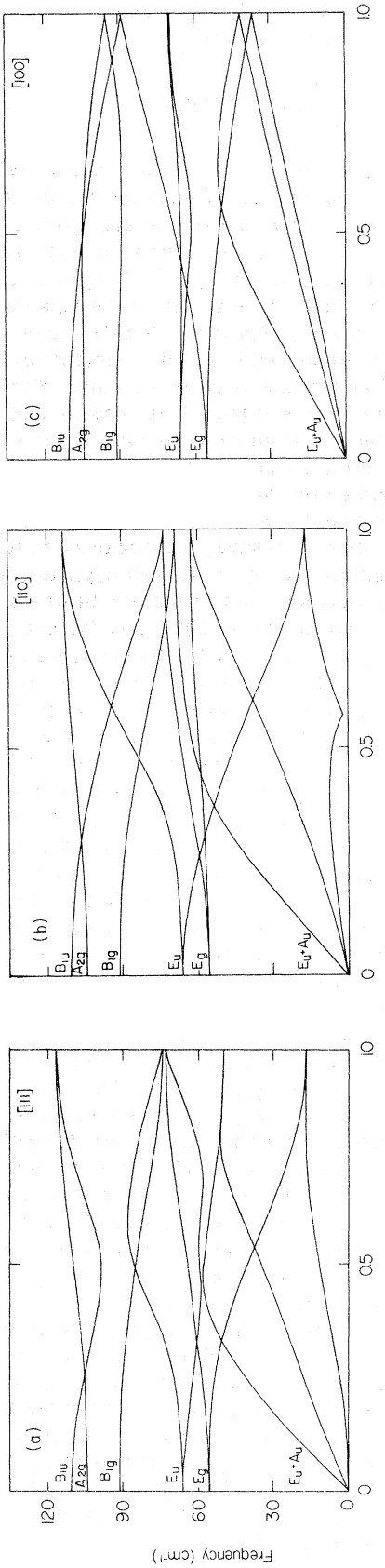

FIG. 3. Dispersion curves for γ-N_2 at unit-cell parameters. $a=b=3.94$ Å, $c=5.08$ Å corresponding to a calculated external pressure of 4 kbars. (a) [111] direction; (b) [110] direction; (c) [100] direction.

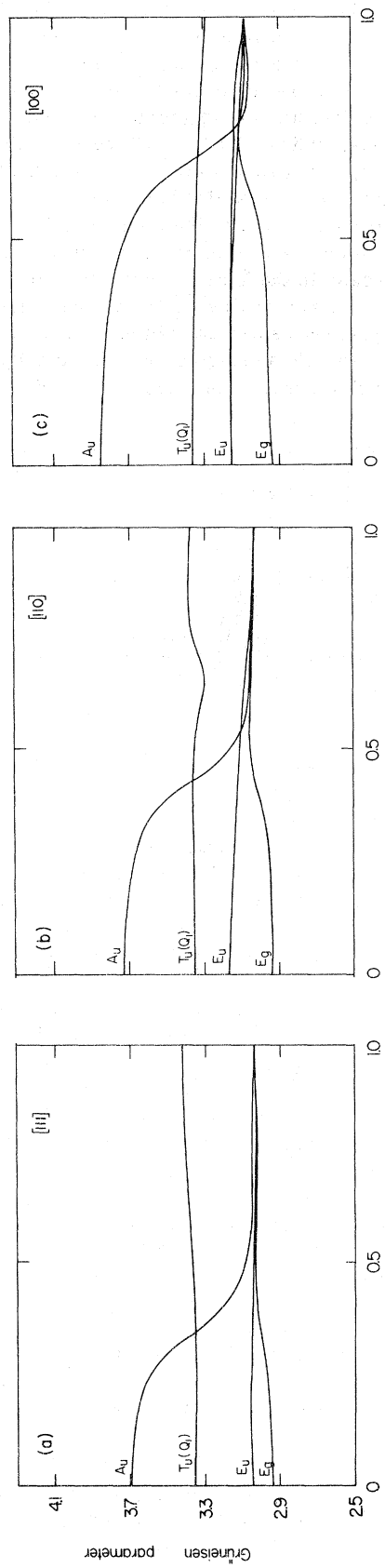

FIG. 4. Dispersion of the Grüneisen mode parameters for α-N_2. The three acoustical modes (A_u and E_u at $\vec{k}=0$) and two optical modes (T_u and E_g at $\vec{k}=0$) are shown. (a) [111] direction; (b) [110] direction; (c) [100] direction.

density-of-lattice-states function $D(\omega)$ for α-N_2 and γ-N_2 at various volumes. The standard method was used for a cubic α phase while suitable modifications were introduced into the BZ sampling scheme for treating the tetragonal γ phase. Standard channel widths of 0.25 cm^{-1} were employed. The convergence properties of the calculated density of states were examined by requiring that the calculated nth moment of the frequency $\langle\omega^n\rangle$ will be stable within a prescribed tolerance with respect to an increase in the $\vec{k}$-grid mesh used for sampling the BZ. Since lattice contributions to thermodynamic properties are calculated by performing suitable ensemble averaging over the density of states, such a convergence check will define the accuracy of the calculated thermodynamic properties. We thus compute

$$\langle\omega^n\rangle_{\Delta k_i} = \int_0^\infty D_{\Delta k_i}(\omega)\,\omega^n d\omega, \tag{14}$$

where $D_{\Delta k_i}(\omega)$ denotes the normalized density of states calculated with a $\vec{k}$-grid mesh indicated by $\Delta k_i (i = x, y,$ and z in the reciprocal-space unit-cell axis) for $-2 < n < 20$. We require that the largest difference $(\langle\omega^n\rangle_{\Delta k_i^c} - \langle\omega^n\rangle_{\Delta k_i})/\langle\omega^n\rangle_{\Delta k_i^c}$ (where Δk_i^c denotes the highest $\vec{k}$-grid mesh) be less than 1% for all moments. Around $\vec{k}=0$ a fixed grid of 190 $\vec{k}$ points is employed to avoid numerical errors introduced by the interpolation scheme. For low-temperature crystal phases such as α- and γ-N_2 (transition temperature to the disordered high-temperature β phase being 36.5–50 °K for pressure lower than 6 atm) such a stability of the -2 to 20th moments against an increase in the $\vec{k}$-grid mesh, should suffice to assure good accuracy in the calculated lattice free energy, heat capacity, and root-mean-square amplitudes of vibrations. It was observed that the use of 1007 inequivalent $\vec{k}$ points in the BZ and a mesh of 190 points around the vicinity of $\vec{k}=0$ assures the convergence of the Debye temperature to within less than 10^{-3}% for the first moment and 10^{-2}% for the 20th moment. A similar accuracy was obtained for the γ-N_2 density of states. For smaller unit-cell volumes a somewhat lower accuracy was obtained for the high moments, e.g., 4.6×10^{-2}% for the 20th moment of α-N_2 at unit-cell dimension of 5.40 Å (corresponding to a pressure of 4 atm at $T=0$ °K). This accuracy is considered sufficient for our purpose, and subsequently this grid was used in further calculations. The density of states calculated with convergent $\vec{k}$ grids for α-N_2 and γ-N_2 are given in Fig. 5 for several densities.

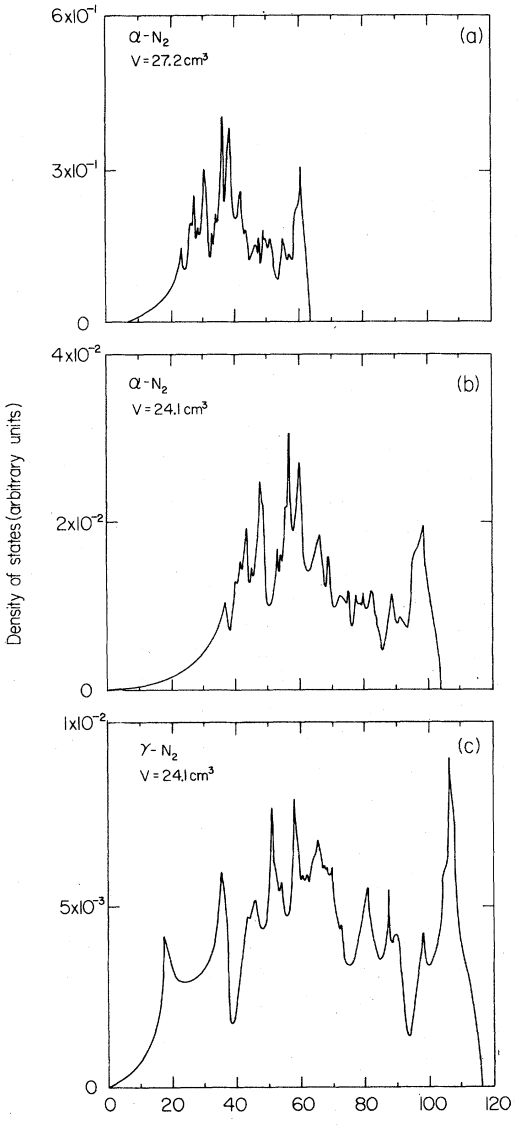

FIG. 5. Density of states of α- and γ-N_2. (a) α-N_2 at $V=27.2$ cm^3; (b) α-N_2 at $V=24.1$ cm^3; (c) γ-N_2 at $V=24.1$ cm^3.

The highest-frequency peak in both α- and γ-N_2 is contributed by the high-energy modes that are translations at the Γ point. The doublet in the α-N_2 density of states at around 30–40 cm^{-1} at zero pressure and at 55–60 cm^{-1} at 4 kbars are contributed by lattice modes that are pure rotations at $\vec{k}=0$. The increase in pressure tends to shift the whole spectrum almost uniformly to higher frequencies although the low-frequency part is slightly less shifted.

It has been previously commented by several authors that it is desirable to obtain an effective Debye temperature from a detailed real-solid density-of-states calculations in order to facilitate calculations of properties such as the Mössbauer recoiless fraction[28–30] and heat capacity.[31] Figure 6 reveals the dependence of the Debye temperature $\Theta_D^{(n)}$ calculated from the nth moment of the frequency, on n.

$$\Theta_D^{(n)} = (h/k_B)[\tfrac{1}{3}(n+3)\langle\omega^n\rangle]^{1/n}, \quad n > -3 \; n \neq 0. \quad (15)$$

$\Theta_D^{(n)}$ is the cutoff temperature of a Debye distribution having the same nth moment as the real $D(\omega)$. Similar plots for rare-gas solids[32] indicate a variation of less than 2% in $\Theta_D^{(n)}$ in the range $-2 < n < 4$. In a molecular solid such as α-N_2 the large number of optical branches introduce strong deviations from a Debye spectrum, resulting in a rapid variation of $\Theta_D^{(n)}$ for low n.

This "fitting" of an actual density of state to a Debye model in molecular crystals having a relatively large number of optical branches requires some comments. It can be easily seen that the "normalized" nth moment in the Debye model with a characteristic cutoff frequency ω_D^{n-1} is

$$\langle\omega_D^n\rangle/\langle\omega_D^1\rangle^n = \tfrac{1}{3}(n+3)(\tfrac{3}{4})^n, \quad \langle\omega_D^n\rangle = \tfrac{1}{3}(n+3)\,\omega_D^n \quad (16)$$

and does not depend neither on the crystal space group nor on the crystal density. These simplifications, inherent in the Debye model, are not satisfied in actual calculations for molecular solids where a large part of the density of states is contributed by the optical branches that have an involved frequency dependence. Furthermore, the fitting of an actual density of states to a Debye density of states by minimizing the sum of differences

$$\sum_n (\langle\omega^n\rangle - \langle\omega_D^n\rangle)^2$$

is divergent as n increases. This can be viewed from Fig. 7 where the ratio $(\langle\omega^n\rangle/\langle\omega^1\rangle^n/(\langle\omega_D^n\rangle/\langle\omega_D^1\rangle^n)$ vs n is plotted for several volumes of α-N_2 and for γ-N_2. It is seen that while for the lowest values of n (which give more weight to the density at low frequencies) the ratio is close to unity, it diverges strongly for large n, the deviation increasing with decreasing volume. It is therefore evident that in calculating thermodynamic properties of molecular solids such as root-mean-square amplitude, zero-point energy, specific heat, etc., by expanding the corresponding integral over the density of states in power series of the various frequency moments[33(b)] one should avoid using a Debye density of states that strongly underestimates high-frequency moments.

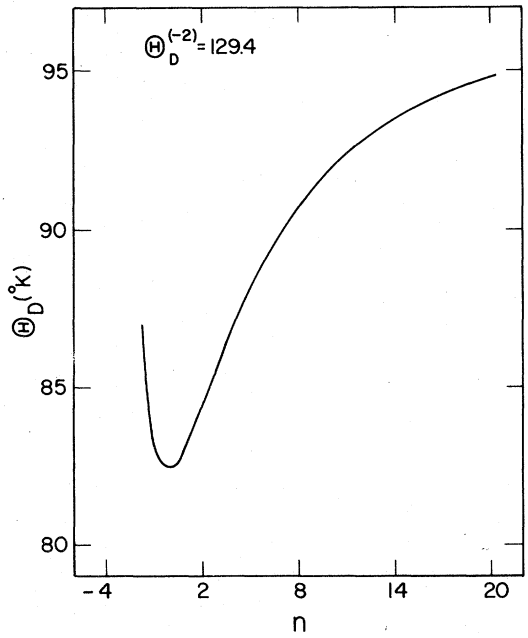

FIG. 6. Variation of $\Theta_D^{(n)}$ calculated from the nth moment of the real density of states $D(\omega)$ for α-N_2.

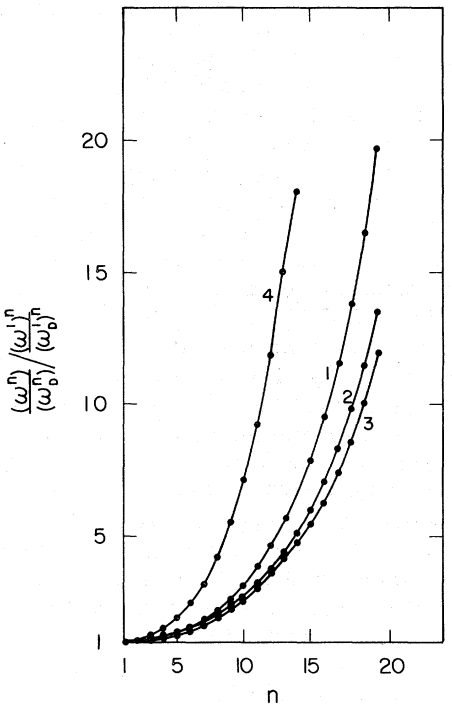

FIG. 7. Normalized moment ratio for the exact and Debye model calculations α-N_2, $a = 5.40$ Å; α-N_2, $a = 5.63$ Å; α-N_2, $a = 5.67$ Å; γ-N_2, $a = b = 3.94$ Å, $c = 5.10$ Å.

The calculations presented here also suggest that the Debye model might be used to determine properties that depend on low and positive moments of frequency such as the high-temperature limit of the specific heat, while it should be less adequate for calculating the low-temperature heat capacity and the high-temperature root-mean-square amplitudes that depend on the negative frequency moments. The approximation made in the Debye model that the solid is an elastic continuum is thus unjustified for solid properties that are related to high momonts where the discrete structure of the solid should be explicitly considered.

To compare our calculated values of Θ_D with ex-

periments the most common choice of Domb and Salter[33] $\omega_{DS}^2 = \langle\omega^2\rangle$ is employed.

Experimental determination of Θ_D for the α phase are: 68 °K at $T = 20$ °K, 73 °K at[34] 10 °K and 80.6° at the lowest temperature measured $T = 4.2 = 4.2$ °K.[35] Our calculation yields $\Theta_D = 84.4$ °K at the unit-cell volume corresponding to equilibrium at $T = 0$ °K, in good agreement with the value of Bagatoskii *et al.*[35] Using the linear expansion coefficient determined experimentally by Bolz *et al.*,[9] the calculated Θ_D at the unit-cell volume corresponding to 20 °K is 75.3 °K, in reasonable agreement with the experimental data.[34]

Schuch and Mills[10] have estimated Θ_D in computing the experimental Debye-Waller factor for γ-N_2, using the de Boer reduced equation of state[36] as an interpolation scheme, obtaining $\Theta_D = 94$ °K. Our calculated value of 125.0 °K is considerably higher and provides a better approximation. A lower Debye-Waller factor is thus predicted by the present calculation. It should be noted that our calculation of the volume dependence of the Debye temperature $\Theta_D(V)$ predicts similar values for the α and the γ phases at the same volume, in agreement with the approximation made by Raich[37] in calculating α-to-γ phase transition.

V. THERMAL EXPANSION

The density of states $D(\omega)$ is used to compute the thermal-expansion coefficient of α-N_2. This is done by minimizing the total crystal free energy $F(a, T)$ (where a denotes the unit-cell parameter), for various values of (a, T). The free energy is given

$$F(a,T) = \Phi_s(a) + \tfrac{1}{2}\hbar_B \int_0^\infty D(\omega,a)\omega\, d\omega + kT\int_0^\infty D(\omega,a)\ln(1 - e^{-\hbar\omega/kBT})\, d\omega. \quad (17)$$

$\Phi_s(a)$ is the static energy calculated by performing the appropriate lattice sums on the pair potential $V(r_{ij})$ [Eqs. (4)–(6)]. It has been previously shown[5] that summation of the contribution of 5^3 unit cells relative to a central unit cell, suffices to assure the convergence of $\Phi_s(a)$ to within less than 0.1%. The second and third terms in Eq. (17) denote the zero-point energy and the lattice thermal energy, respectively. The contribution of the intramolecular modes to these terms is neglected since these modes (of frequency 2300 cm^{-1} for α-N_2) are only slightly populated below the α-β transition temperature and thus contribute negligibly to the thermal expansion. The last two terms in Eq. (17) are calculated numerically from the density of states. Minimization of the static energy alone with respect to the unit-cell volume has been shown to yield a unit-cell parameter of $a = 5.63$ Å while addition of the zero-point-energy term to the minimization procedure was shown to increase this value to 5.66 Å.[5] Zero-point-energy contributions have been calculated self-consistently using $D(\omega, a)$ at the unit-cell parameter that minimizes the first two terms in Eq. (17). Minimization of $F(a, T)$ yields the function $a(T)$. The results are plotted in Fig. 8 in units of $a_0 \equiv a(T = 0)$. Fitting to the relation $a/a_0 = 1 + \eta T$ yields an average linear thermal-expansion coefficient of $\eta \sim 2.8\times10^{-4}$ °K^{-1} for $0 < T < 20°$. This agrees reasonably well with the rough experimental estimation of $\eta \sim 2\times10^{-4}$ °K^{-1} for $4.2 < T < 20$ °K.

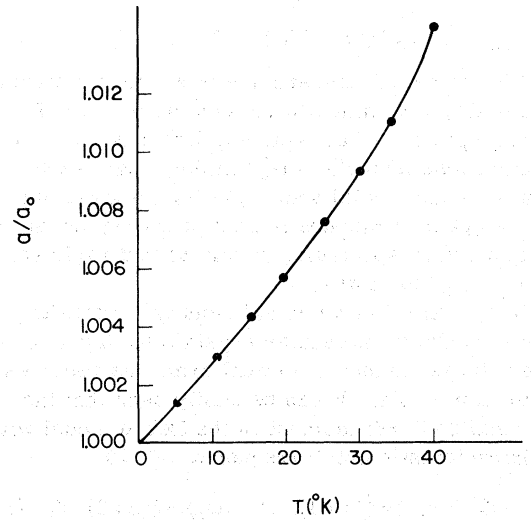

FIG. 8. Calculated temperature dependence of the α-N_2 unit-cell parameter.

It should be noted that the zero-point-energy term could be calculated to a very good approximation from the $\vec{k} = 0$ mode frequencies without the detailed knowledge of the density of states.[5] This could be done by using an Einstein model for each of the optical branches with its appropriate frequency at $\vec{k} = 0$, and a Debye model for the acoustic branches using an acoustic Debye temperature that is determined from the lowest optical frequency. This yields a zero-point energy of 0.4138 and 0.3127 kcal/mole for α-N_2 at unit-cell volumes of 41 $Å^3$ and 44.6 $Å^3$/molecule, respectively, compared with 0.4097 and 0.3112 kcal/mole obtained from a direct evaluation from the density of states using a low grid mesh of 226 points, and 0.4086 and 0.3124 kcal/mole obtained with a higher grid mesh of 871 points. Since the evaluation of $D(\omega)$ for polyatomic molecular crystals is usually difficult to implement in practice,[38] such an approximation to the zero-point energy and its volume dependence could be useful in calculating cohesive energies, conformations at dynamical equilibrium, and low temperatures.

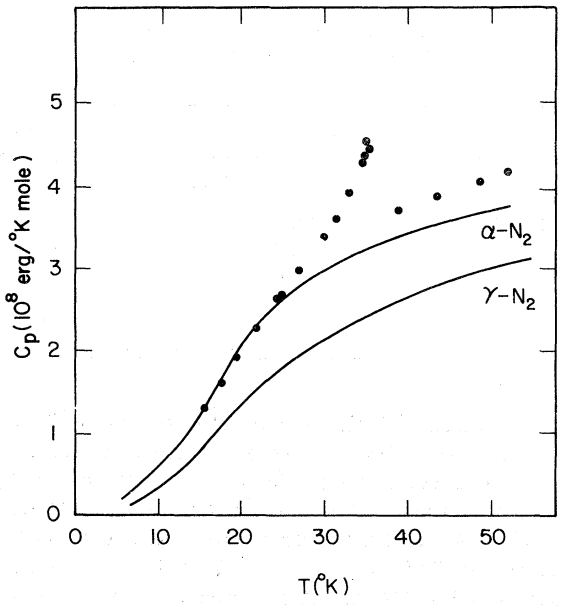

FIG. 9. Heat capacity of α- and γ-N_2. The α-N_2 values are calculated at the equilibrium zero-pressure conformation ($V=27.2$ cm^3), and the γ-N_2 values are calculated at equilibrium under a pressure of 4 kbars ($V=24.1$ cm^3). Points indicate the experimental data of Giauque and Clayton (Ref. 11) for α-N_2.

VI. HEAT CAPACITY

Next, we turn to the calculation of the lattice contribution to the heat capacity of α- and γ-N_2. The heat capacity at constant pressure is

$$C_P(T) = 5N_0 \int_0^\infty D(\omega) C(\omega, T)\, d\omega + 9\eta^2 BVT, \quad (18)$$

where $C(\omega, T)$ is the heat capacity of a harmonic oscillator having a frequency ω, N_0 is Avogadro's number, $5N_0$ is the total number of degrees of freedom (two librations and three translations for each molecule), B is the bulk modulus, and V is the molar volume. Using the experimental estimate[39] to B (10^{10}–10^{11} erg. cm^{-3}) with the experimental linear-expansion coefficient η and molar volume V, the second term in Eq. (13) is estimated to be small relative to the first term, and consequently can be neglected. The thermal-expansion effects on $D(\omega)$ are likewise small and may be safely neglected. The calculated heat capacity as a function of temperature of α-N_2 at zero pressure, and of γ-N_2 at a molar volume of 24.1 cm^3 corresponding to a pressure of 4 kbars, are shown on Fig. 9, together with the experimental points of Giauque *et al.*[11] for α-N_2 above 16 °K. The calculated and experimental results agree fairly well below 27 °K. Above this temperature the agreement becomes worse owing to the increase in lattice anharmonicity accompanying the α-to β phase transition at 35.6 °K. The γ-N_2 heat capacity is considerably lower than the corresponding α-N_2 values owing to its higher density of states at the high-frequency part of the spectrum that is relatively unpopulated at low temperatures. Presently, no experimental data on the γ-N_2 heat capacity and on the low-temperature α-N_2 heat capacity, are available.

VII. AMPLITUDE OF VIBRATION

The amplitudes of vibrations of α-N_2 were calculated directly from the displacement-correlation function[40]

$$\langle u_\lambda(lt) u_{\lambda'}(l't')\rangle = \frac{H}{2N(M_t M_{t'})^{1/2}} \sum_{\vec{k},j} e_\lambda(t \mid \vec{k}j) \times e_{\lambda'}(t' \mid kj) \coth h\omega_j(\vec{k})/2k_B T, \quad (19)$$

using the eigenvectors $\vec{e}(t \mid \vec{k}, j)$ of the lattice frequencies calculated at N points in the Brillouin zone. The summation over j in Eq. (19) is performed over all the branches, and the acoustical modes at $\vec{k}=0$ are excluded. A dense sampling of points in the Brillouin zone was taken so as to assure the convergence of the sum in Eq. (6). The results of the calculations using Eq. (19) satisfy the relation

$$\langle u_x u_x\rangle = \langle u_y u_y\rangle = \langle u_z u_z\rangle, \quad \langle u_x u_y\rangle = \langle u_y u_z\rangle = \langle u_z u_x\rangle. \quad (20)$$

The values of $\langle u_i u_j\rangle$ at different temperatures are given in columns 2 and 3 of Table II. Column 4 shows the components of the amplitude of vibration along the molecular axis, which is given by

$$\langle u_l\rangle = (u_{11} + 2u_{12})^{1/2},$$

column 5 gives the component of the displacement along each one of the two principal axis perpendicular to the molecular axis

$$\langle u_t\rangle = (u_{11} - u_{12})^{1/2}.$$

It is difficult to estimate how much of the thermal motion is due to rotation of the molecule and how much is due to the translation of its center of mass. However, assuming, as did La Placa and Hamilton,[41] that the translational motion is isotropic,

TABLE II. Thermal parameters, root-mean-square displacements, and estimate of amplitude of libration of α-N_2.

T (°K)	$\langle u_{ii}^2\rangle$ (Å^2)	$\langle u_i u_j\rangle$ (Å^2)	$\langle u_l\rangle$ (Å)	$\langle u_t\rangle$ (Å)	$\langle\Theta\rangle$ (deg)
4°K	0.0315	−0.0080	0.124	0.198	17.7
10°K	0.0409	−0.0124	0.129	0.230	21.8
15°K	0.0514	−0.0150	0.146	0.257	24.3
20°K	0.0614	−0.0190	0.153	0.283	27.3
25°K	0.0726	−0.0230	0.163	0.309	30.1
36°K	0.1020	−0.0301	0.204	0.360	34.4

u_l can be associated with the translation, and $\langle\Theta\rangle = 2(\sqrt{3}U_{12}/l)$, where l is the length of the N_2 molecule, represents the root-mean-square angular displacement (in radians) for each one of the two librational degrees of freedom.

The values for librational motion given in Table II are in agreement with the x-ray results of La Placa and Hamilton, who reported a value of 17° at 20 °K.

In conclusion, our results for the mean-square-amplitude displacements confirm the approximated calculation of Cahill and LeRoi[42] and Goodings and Henkelman,[43] and point out that anharmonicity could be important in the librational motions of α-N_2.

VIII. COMPARISON WITH SELF-CONSISTENT PHONON TREATMENT

Raich *et al.*[23] have recently performed a self-consistent phonon (SCP) treatment[44] of solid α-N_2 using a different 12-6 potential. As a comparison between the SCP and the quasiharmonic (QH) results the above-mentioned authors presented the lattice frequencies at $\vec{k}=0$ as computed by both methods using the same potential, however the experimental unit-cell dimensions were used for the QH treatment ($a=5.649$ Å); while for the SCP treatment the predicted theoretical value ($a=5.714$ Å), was employed. Previous SCP calculations we were performed only on atomic crystals. We thus briefly comment on the relation between QH and SCP results for the molecular solid studied here at $T=0$ °K.

The basic methodology used in SCP theory is to incorporate anharmonic effects to first order by replacing the QH force constants of Eq. (13) by an appropriate ensemble average over a function related to the displacement-correlation tensor. On the other hand, anharmonic effects are partially introduced in the QH scheme by calculating the lattice-dynamical properties at the atomic positions that minimize the frequency-dependent free energy. At $T=0$ °K, this reduces to the modification in the lattice frequencies owing to the changes in atomic positions induced by zero-point effects. Thus in the QH approach one assumes that the collective effect of all lattice mode is to renormalize the dynamical variables generating thereby a new set of *fixed* atomic positions at which the force constants are to be evaluated; in the SCP method, *an ensemble average* is used. Since the ensemble average yields a larger force constant than the discrete force constant obtained at a given unit-cell parameter a, one gets $\omega_j^{SCP}(a) > \omega_j^{QH}(a)$ for a given value of a.[45] On the other hand, the *equilibrium* lattice parameter a_{SCP} calculated by minimizing the SCP free energy, is usually larger than the corresponding value a_{QH} calculated in the QH approximation.[46] This tends to decrease the $\omega_j^{SCP}(a_{SCP})$ relative to $\omega_j^{QH}(a_{QH})$. To investigate in more detail these conflicting effects we repeated our QH calculation using the potential employed by Raich *et al.*[23] A careful minimization of the total lattice energy at $T=0°$ yielded $a_{QH}=5.62$ Å as compared with $a_{SCP}=5.714$ Å. The frequencies at $\vec{k}=0$ obtained by us at this a_{QH} value are compared with the frequencies obtained by Raich *et al.* in a SCP treatment at a_{SCP} in Table III. The weighted deviation

$$\gamma = \sum_{i=1}^{3\sigma-5} \left| \omega_i^{QH} - \omega_i^{SCP} \right|$$

is only 0.95 cm^{-1}°.[47] The dispersion curves calculated by the QH method have exactly the same shape as those obtained by SCP calculation, since the averaging procedure used by the latter method removes almost completely all the $\vec{k}$ dependence of the anharmonic corrections. Similarly, the binding energy calculated by the SCP method is 1.58 kcal/mole, while that calculated by the QH method is 1.56 kcal/mole.

TABLE III. Comparison between self-consistent phonon and quasiharmonic frequencies each calculated at the minimum of the corresponding free energy at 0 °K. Values given in cm^{-1}.

Mode	$\omega_j^{SCP}(a_{SCP})$	$\omega_j^{QH}(a_{QH})$
T_u	70.1	70.8
E_u	52.0	53.2
T_g	47.6	47.8
T_u	48.8	47.8
A_u	44.3	44.1
T_g	40.8	39.3
E_g	36.7	35.2

We thus conclude that if one follows *consistently* the QH scheme, reasonably accurate frequencies can be obtained owing to the nearly cancelling effects of the increase in the lattice frequencies at fixed volume and the increase in equilibrium volume in going from QH to SCP approximation. For more accurate determination of the lattice parameter at equilibrium and behavior at higher temperatures, SCP methods can not be avoided.

IX. SUMMARY

The previously published, interaction potential between N_2 molecules was used to compute the lattice-mode frequencies of α- and γ-N_2 crystals at the equilibrium structure corresponding to various pressures. Dispersion curves as well as density of lattice modes are given for both phases. These are used to compute the lattice heat capacity, root-mean-square amplitudes of vibrations, dispersion of Grüneisen mode parameters, linear

thermal-expansion coefficients, and the Debye temperatures. Reasonable agreement is obtained with experimental data whenever experimental data are available. More intensive examination of the proposed calculations would be possible when more experimental data such as neutron scattering (coherent elastic and incoherent inelastic) and crystallographically determined amplitude of vibration would be available.

The calculation of the dynamical properties of molecular crystals do not pose any serious difficulty relative to the more familiar atomic crystals calculations. The marked differences in the calculation schemes are the following.

(a) In calculations on molecular crystals of arbitrary conformation, one should take special care with the problem of relaxing all forces and torques exerted by the crystal field on the molecules. Because of the anharmonicity of the crystal potential, residual forces and torques have a marked effect on the calculated lattice frequencies.

(b) Because of the presence of a relatively large number of optical modes in the molecular crystal lattice spectrum, the lattice zero-point energy contributes a significant part to the free energy at low temperatures. Optimization of the crystal structure for a given interaction potential, should take zero-point effect into account. Because of the high ratio between the number of optical to acouttical branches characterizing molecular crystals, the lattice spectrum deviates significantly from a Debye-type spectrum. A Debye model is thus inaddequate for computing thermodynamical properties that involve high-frequency moments.

In view of the practical possibility of computing lattice properties for a given molecular potential, it seems that such calculation should provide a good test to the quality of the interaction potential. Substantial effort has been lately devoted to the calculation of interaction potential from first principles,[48–50] and from combinations of first principle and empirical data.[51] The quality of these potentials has been examined by calculating virial coefficients and viscosity[41] or lattice cohesive energies.[49] We believe that calculations of lattice-dynamical properties in the corresponding crystals would provide a much better examination of the anisotropy and detailed characteristics of such interaction potentials.[52]

ACKNOWLEDGMENTS

The authors are grateful to Professor G. Gilat and Professor M. L. Klein for helpful discussions and comments.

*Present address: Dept. of Physics, Northwestern University, Evanston, Ill. 60201.

[1]G. S. Pawley, Phys. Status Solidi 20, 347 (1967).
[2]A. Warshel and S. Lifson, J. Chem. Phys. 53, 582 (1970).
[3]P. A. Reynolds, J. Chem. Phys. 59, 2777 (1973).
[4]G. Filippini, C. M. Gramaccioli, M. Simonetta, and G. B. Suffritti, J. Chem. Phys. 59, 5088 (1973).
[5]A. Zunger and E. Huler, J. Chem. Phys. 62, 3010 (1975).
[6]G. Taddei, H. Bonadeo, M. P. Marzocchi, and S. Califano, J. Chem. Phys. 58, 966 (1973).
[7]A. A. Maradudin, E. W. Montroll, G. H. Weiss, and I. P. Ipatova, *Theory of Lattice Dynamics in the Harmonic Approximation* (Academic, New York, 1971).
[8]G. Gilat and L. J. Raubenheimer, Phys. Rev. 144, 390 (1966); and 157, 586 (1967).
[9]L. H. Bolz, M. E. Boyd, F. A. Mauer, and H. S. Pieser, Acta. Crystallogr. 12, 247 (1959).
[10]A. F. Schuch and E. L. Milles, J. Chem. Phys. 52, 6000 (1970).
[11]W. F. Giauque and J. O. Clayton, J. Am. Chem. Soc. 54, 4875 (1933).
[12]K. K. Kelly, Bureau of Mines, Report No. 389, Washington, D. C. (1962) (unpublished).
[13]A. Ron and O. Schnepp, J. Chem. Phys. 46, 3991 (1967).
[14]A. Anderson and G. E. Leroy, J. Chem. Phys. 45, 4359 (1966).
[15]A. Anderson, T. S. Sun, and M. D. A. Donkersloot, Can. J. Phys. 48, 2265 (1970).
[16]M. Brit, A. Ron, and O. Schnepp, J. Chem. Phys. 51, 1318 (1969).
[17]F. D. Medina and W. B. Daniels, J. Chem. Phys. 59, 6175 (1973).
[18]I. N. Levine, J. Chem. Phys. 45, 827 (1966).
[19]J. K. Kjems and G. Dolling, Phys. Rev. B 11, 1639 (1975).
[20]C. A. Swenson, J. Chem. Phys. 23, 1963 (1955).
[21]A. D. Woods, Phys. Rev. 131, 1076 (1963).
[22]A. Ron and O. Schnepp, Discuss. Faraday Soc. 48, 26 (1970).
[23]J. C. Raich, N. S. Gillis, and A. B. Anderson, J. Chem. Phys. 61, 1399 (1974).
[24]T. Luty and G. S. Pawley, Chem. Phys. Lett. 28, 593 (1974).
[25]F. D. Medina and W. B. Daniels, Phys. Rev. Lett. 32, 167 (1974).
[26]M. M. Thiery, D. Fabre, M. J. Louis, and H. Vu, J. Chem. Phys. 59, 4559 (1973).
[27]V. Chandrasekharan, D. Fabre, M. M. Thiery, E. Uzan, M. C. A. Donkersloot, and S. H. Walmsley, Chem. Phys. Lett. 26, 284 (1974).
[28]K. Mahesh, J. Phys. Soc. Jpn. 28, 818 (1970).
[29]K. Mahesh and S. V. Kapil, Phys. Status Solidi B 47, 397 (1971).
[30]S. S. Nandwani, D. Raj, and S. P. Puri, J. Phys. C 4, 1929 (1971).
[31]K. Mahesh, Phys. Status Solidi 61, 695 (1974).
[32]J. Skalyo, V. J. Minkiewicz, G. Shirane, and W. B. Daniels, Phys. Rev. B 6, 4766 (1971).
[33](a) C. Domb and L. S. Salter, Philos. Mag. 43, 1083 (1952). (b) E. L. Pollock, T. A. Bruce, G. V. Chester, and J. A. Krumhansl, Phys. Rev. B 5, 4180 (1972).
[34]Landolt-Börnstein, *Zahlenwerte and Funktionen* (Springer, Berlin, 1961), Vol. 2, p. 405.

[35]M. I. Bagatoskii, V. A. Kucheryavy, V. G. Manzhelii, and V. A. Popov, Phys. Status Solidi 26, 453 (1968).
[36]L. Jansen, A. Michels, and J. M. Lupton, Physica 20, 1235 (1954).
[37]J. C. Raich and R. L. Mills, J. Chem. Phys. 55, 1811 (1971).
[38]P. J. Grout and J. W. Leech, J. Phys. C 7, 3245 (1974).
[39]No data for N_2. Data for benzene: J. C. W. Hoseltine, D. W. Elliott, and O. B. Wilson, J. Chem. Phys. 40, 2584 (1964).
[40]A. A. Maradudin, E. W. Montroll, G. H. Weiss, and I. P. Ipatova, *Theory of Lattice Dynamics in the Harmonic Approximation* (Academic, New York, 1971), p. 62.
[41]S. J. La Placa and W. H. Hamilton, Acta Crystallogr. B28, 984 (1972).
[42]J. E. Cahill and G. E. LeRoi, J. Chem. Phys. 51, 1324 (1969).
[43]D. A. Goodings and M. Henkelman, Can. J. Phys. 49, 2898 (1971).
[44]For general reviews, see (a) M. L. Klein and G. K. Horton, J. Low Temp. Phys. 9, 151 (1972); (b) N. R. Werthamer, Am. J. Phys. 37, 763 (1969); (c) N. R. Werthamer, Phys. Rev. B 1, 572 (1970).
[45]Bohlin, J. Phys. Chem. Solids 29, 1805 (1968).
[46]M. L. Klein, V. V. Goldman and G. K. Horton, J. Phys. Chem. Solids 31, 7441 (1970).
[47]For comparison, the QH results of Raich *et al.* (Ref. 23) at $a = 5.649$ Å were reproduced by our program to within $\lambda = 0.43$ cm^{-1}.
[48]V. Magnasco and G. F. Musso, J. Chem. Phys. 47, 1723 (1967); 47, 4617 (1967); 47, 4629 (1967).
[49]R. G. Gordon and Y. S. Kim, J. Chem. Phys. 56, 3122 (1972).
[50]C. F. Bader, H. F. Schaefer, and P. A. Kollman, Mol. Phys. 24, 235 (1972).
[51]A. J. Thakkar and H. Smith, Chem. Phys. Lett. 24, 157 (1974).
[52]A. Zunger, Mol. Phys. 28, 713 (1974).